

## YCa<sub>4</sub>O(BO<sub>3</sub>)<sub>3</sub> (YCOB) high temperature vibration sensor

Kyungrim Kim, Shujun Zhang, Wenbin Huang, Fapeng Yu, and Xiaoning Jiang

Citation: *J. Appl. Phys.* **109**, 126103 (2011); doi: 10.1063/1.3598115

View online: <http://dx.doi.org/10.1063/1.3598115>

View Table of Contents: <http://jap.aip.org/resource/1/JAPIAU/v109/i12>

Published by the [American Institute of Physics](#).

---

### Related Articles

A simply constructed but efficacious shock tester for high-g level shock simulation  
*Rev. Sci. Instrum.* **83**, 075115 (2012)

Directional anemometer based on an anisotropic flat-clad tapered fiber Michelson interferometer  
*Appl. Phys. Lett.* **101**, 023502 (2012)

Measurement of fast-changing low velocities by photonic Doppler velocimetry  
*Rev. Sci. Instrum.* **83**, 073301 (2012)

Note: Frequency-conversion photonic Doppler velocimetry with an inverted circulator  
*Rev. Sci. Instrum.* **83**, 026109 (2012)

Optic-microwave mixing velocimeter for superhigh velocity measurement  
*Rev. Sci. Instrum.* **82**, 123114 (2011)

---

### Additional information on *J. Appl. Phys.*

Journal Homepage: <http://jap.aip.org/>

Journal Information: [http://jap.aip.org/about/about\\_the\\_journal](http://jap.aip.org/about/about_the_journal)

Top downloads: [http://jap.aip.org/features/most\\_downloaded](http://jap.aip.org/features/most_downloaded)

Information for Authors: <http://jap.aip.org/authors>

## ADVERTISEMENT



The advertisement banner features a green and white background with abstract, flowing lines. At the top center, the text "AIP Advances" is displayed in a green, sans-serif font, with a series of orange and yellow circles of varying sizes arranged in an arc above it. Below this, the text "Special Topic Section:" is written in a smaller, white font, followed by "PHYSICS OF CANCER" in a large, bold, white font. At the bottom left, the text "Why cancer? Why physics?" is written in a green font. At the bottom right, there is a blue button with the text "View Articles Now" in white.

**YCa<sub>4</sub>O(BO<sub>3</sub>)<sub>3</sub> (YCOB) high temperature vibration sensor**Kyungrim Kim,<sup>1</sup> Shujun Zhang,<sup>2</sup> Wenbin Huang,<sup>1</sup> Fapeng Yu,<sup>2</sup> and Xiaoning Jiang<sup>1,a)</sup><sup>1</sup>*Department of Mechanical and Aerospace Engineering, North Carolina State University, Raleigh, North Carolina 27695, USA*<sup>2</sup>*Materials Research Institute, Pennsylvania State University, University Park, Pennsylvania 16802, USA*

(Received 7 April 2011; accepted 10 May 2011; published online 22 June 2011)

A shear-mode piezoelectric accelerometer using YCa<sub>4</sub>O(BO<sub>3</sub>)<sub>3</sub> (YCOB) single crystal was designed, fabricated and successfully tested for high temperature vibration sensing applications. The prototyped sensor was tested at temperatures ranging from room temperature to 1000 °C and at frequencies ranging from 80 Hz to 1 kHz. The sensitivity of the sensor was found to be 5.7 pC/g throughout the tested frequency and temperature range. In addition, YCOB piezoelectric accelerometers remained the same sensitivity at 1000 °C for a dwell time of four hours, exhibiting high stability and reliability. © 2011 American Institute of Physics. [doi:10.1063/1.3598115]

High temperature sensors are essential parts of structural health monitoring to ensure high performance and efficiency in structures such as turbine engines, internal combustion engines and electric generation plants. The sensors for these applications need to be designed so that they can work properly at high temperatures (>1000 °C) for a duration time up to 100 000 h.<sup>1–4</sup> During the past decade, many kinds of sensors such as thermocouples, platinum (Pt) strain gauges, silicon carbide (SiC) sensors, and fiber optic sensors have been developed for high temperature applications. Further advancement in order to obtain simple sensor structures with high sensitivity, high stability, long lifetime and higher operation temperature range has been actively investigated.<sup>4–11</sup> In particular, thin film electrodes (~100 nm thickness), which are capable of withstanding high temperature operations, are crucial needs for high temperature sensors.<sup>12,13</sup> Various thin film electrodes including Pt/Zr, Ir/TiAlN, IrO<sub>2</sub>/Ti, Pt/Ir, and Pt/Rh have been developed for high temperature applications. Nonetheless, their operating temperature is limited by degradation, such as high temperature oxidation and corrosion of thin film electrodes.<sup>14–19</sup> Therefore, high temperature sensors without thin film electrodes are attractive for reliable high temperature applications.

On the other hand, high temperature piezoelectric sensors are of particular interest because they have simple structures, fast response time and easy integration with other parts. However, to date, most existing piezoelectric materials which have been used as sensing elements for high temperature sensors suffer from phase transitions, which can cause degradation of the piezoelectric properties or reduced electrical resistivity at elevated temperatures.<sup>4,5</sup> Recently discovered piezoelectric single crystal yttrium calcium oxyborate YCa<sub>4</sub>O(BO<sub>3</sub>)<sub>3</sub> (YCOB) is known for its stable piezoelectric properties and the absence of phase transitions up to its melting point (~1500 °C). Together with its high resistivity, YCOB has been reported as a promising high temperature sensing crystal.<sup>1,3,4</sup> A high temperature monolithic compression-mode piezoelectric accelerometer using YCOB was fab-

ricated and tested, demonstrating its stable performances at high temperatures up to 1000 °C.<sup>4</sup> In this compression-mode sensor design, a Pt electrode was used, which could potentially cause sensor failure due to electrode degradation. In this letter, an electrodeless shear-mode vibration sensor was designed and fabricated, providing the best overall performance for piezoelectric accelerometer applications at high temperature.

In shear-mode accelerometers, the sensing crystals are clamped or bonded between a center post and seismic masses. Under acceleration, a shear stress from the seismic mass is applied to the sensing crystal, generating a charge signal. By separating the sensing crystals from the base, reduced thermal transient and base bending effects can be obtained in comparison with other types of accelerometers. Furthermore, the electrodeless structure provides more stable performance of the accelerometer at high temperatures because that there is no degradation of thin film electrode at elevated temperatures. Thus, simple and low profile electrodeless shear-mode accelerometers provide many advantages over compression-mode accelerometers.<sup>20–23</sup>

(YXt)-30° cut YCOB single crystals with dimensions of 10 × 12 × 1 mm<sup>3</sup> were fabricated for use as sensing components. The capacitance, resonance frequency and dielectric losses were measured using an impedance analyzer (HP4294 A). The shear mode electromechanical coupling factor ( $k_{26}$ ), elastic compliance ( $s_{66}^E$ ), piezoelectric strain constant ( $d_{26}$ ) and piezoelectric voltage constant ( $g_{26}$ ) were calculated to be 0.22,  $1.8 \times 10^{-11}$  m<sup>2</sup>/N, 10 pC/N, and 0.090 Vm/N respectively, using the following equations<sup>1–3</sup>

$$k_{26}^2 = \frac{\pi f_r}{2f_a} \cot\left(\frac{\pi f_r}{2f_a}\right), \quad (1)$$

$$s_{66}^E = \frac{1}{4\rho t^2 f_a^2 (1 - k_{26}^2)}, \quad (2)$$

$$d_{26}^2 = k_{26}^2 s_{66}^E \epsilon_{22}^T, \quad (3)$$

$$g_{26} = d_{26} / \epsilon_{22}^T. \quad (4)$$

a)Electronic mail: xjiang5@ncsu.edu.

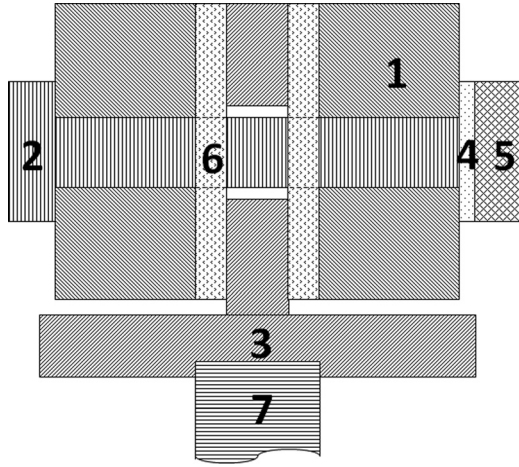


FIG. 1. A schematic cross section of the electroless shear-mode accelerometer sensor.

Figure 1 shows a schematic cross-section of the shear-mode accelerometer. Inconel 601 was chosen as the material for sensor components including seismic masses, housing, and signal wires because of its excellent resistance to high temperature oxidation and corrosion as well as excellent electrical conductivity.<sup>22,23</sup> Four pieces of YCOB crystals (6) are arranged symmetrically on both sides of the center post (3) and they are rigidly secured via the seismic masses (1) by a bolt. The bolt (2), washer (4) and nut (5) clamp seismic masses and YCOB crystals. The clamping torque (0.6 Nm) was applied by the torque control driver (model 285-50, Wiha Quality Tools). One signal wire was welded to the base and another wire was clamped between the nut and the seismic mass directly. The bottom of the center post was bonded to an alumina rod (7) using a type of high temperature adhesive (Resbond 989, Cotronics Corp.). Seismic masses and the center post, which were made of Inconel 601 were electrically and mechanically isolated from each other, thus acted as electrical connections. Since there were no thin film electrodes, and no conductive adhesives on YCOB crystals, the accelerometer was expected to work reliably without the oxidation and corrosion of electrodes at high temperatures. Figure 2 shows an experimental setup for a high temperature test. The sensor was placed in the vertical tube

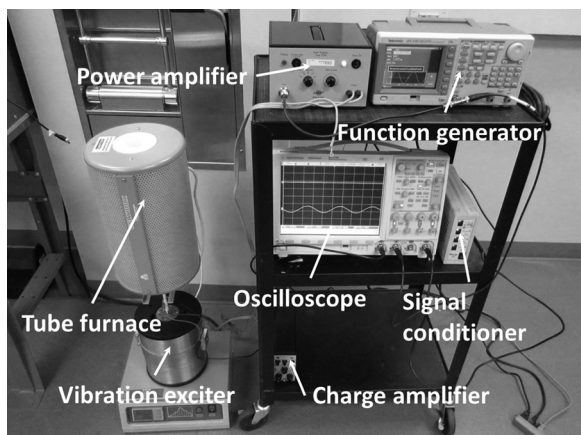


FIG. 2. Experimental setup for high temperature test.

furnace (Model GSL 1100X, MTI Corporation) through an alumina rod. The alumina rod was screwed on a vibration exciter which can provide a maximum force of 178 N (VG 100, Vibration Test Systems, Inc.). The function generator (Model AFG3101, Tectronix) produced a sinusoidal signal and this signal was amplified by a power amplifier (Type 2706, Bruel & Kjaer). Signal was applied to the vibration exciter to generate the desired vibration. The output charge signal from the sensing crystals was converted and amplified to voltage signal through a charge amplifier (Type 2635, Bruel & Kjaer) and monitored by an oscilloscope (Model DSO7104B, Agilent Technologies). At the same time, the acceleration from the vibration exciter was measured by a commercial accelerometer (Model 303A03, PCB Piezotronics), which was attached to the vibration stage of the exciter. This acceleration was recorded on the oscilloscope through a signal conditioner (Model 482A16, PCB Piezotronics). The generated charge from the YCOB device was recorded as a function of temperature (room temperature—1000 °C), vibration frequency (80–1000 Hz), acceleration (1–5 g) and high temperature dwell time at 1000 °C.

The designed device resonance frequency was about 60 kHz; the sensor sensitivity was calculated to be 5.5 pC/g at room temperature and to have frequencies less than 1 kHz using following equations

$$F = ma, \tag{5}$$

$$Q(t) = F(t) \times d_{26}, \tag{6}$$

$$S_Q = Q/a, \tag{7}$$

where  $F$ ,  $m$ ,  $a$ ,  $Q$ ,  $d_{26}$ , and  $S_Q$  are applied inertial force to crystals, seismic masses (= 56 g), applied acceleration (1–5 g), generated charge, piezoelectric coefficient and sensor sensitivity respectively. Figure 3 shows the generated charge of the prototyped electrodeless YCOB accelerometer at room temperature and at frequencies ranging from 80 Hz to 1 kHz. The generated charge from the sensor increased

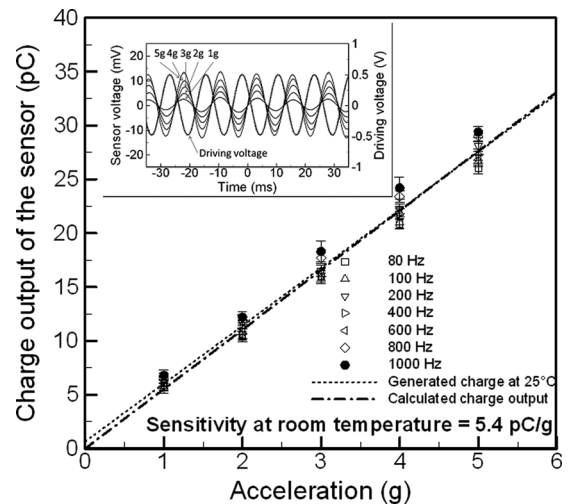


FIG. 3. Comparison of calculated sensitivity and measured sensitivity from the prototyped accelerometer at room temperature in different frequency range. The inset shows the driving voltage signal and the output voltage signal as a function of time.

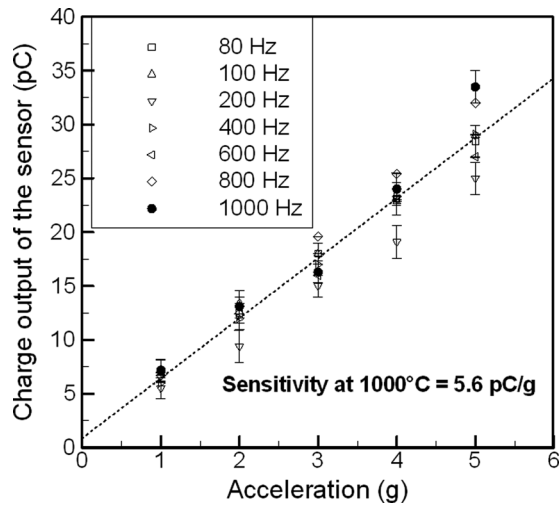


FIG. 4. Sensor charge output as a function of acceleration at 1000 °C.

linearly with the applied acceleration and had a slope of 5.4 pC/g, which corresponded closely with the designed sensitivity (5.5 pC/g). The inset of Fig. 3 shows the driving voltage signal from the function generator and the output voltage signal from the charge amplifier. There is a 180 deg phase shift due to the inverting action of the integrator circuit in the charge amplifier. Figure 4 shows the charge output of the sensor at 1000 °C in different frequency ranges. The sensitivity of the sensor at 1000 °C was found to be 5.6 pC/g, which is close to the room temperature sensitivity. Figure 5 shows the sensitivity of the prototyped sensor with increasing temperatures (25–1000 °C) at the tested frequency range (80–1000 Hz). The sensor sensitivity remained to be reasonably stable in the tested temperature range. The average sensitivity was determined to be 5.7 pC/g throughout the tested frequency and temperature range. Figure 5 inset shows the sensitivity of the prototyped accelerometer measured for 4 h

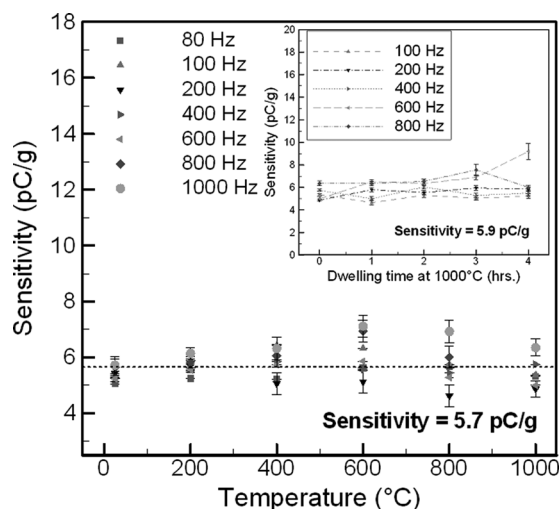


FIG. 5. Sensitivity of the shear-mode accelerometer measured at temperature up to 1000 °C and frequency ranging from 80 to 1000 Hz. The inset shows sensitivity of the shear-mode accelerometer as a function of dwell time at 1000 °C.

at 1000 °C. The average sensitivity of the sensor was found to be 5.9 pC/g during the 4-h dwelling time. Slight sensitivity variation at elevated temperatures might be caused by temperature dependence of the elastic compliance, dielectric permittivity and piezoelectric constant of crystals.<sup>1</sup> The noise due to the heated air flow in the furnace could be another source causing sensitivity variations.

In summary, an electrodeless shear-mode piezoelectric accelerometer using YCOB single crystals was designed, fabricated and tested for high temperature vibration sensing applications. The sensor tests were conducted in frequencies ranging from 80 to 1000 Hz and temperatures ranging from room temperature to 1000 °C. The sensitivity of the accelerometer was found to be 5.4–5.7 pC/g throughout the tested frequency and temperature range. Furthermore, stable sensitivity was observed from the 4-h dwelling test at 1000 °C. More dwelling tests and microscale YCOB sensors will be investigated for further high temperature sensing advancement.

## ACKNOWLEDGMENTS

This project is sponsored by a NC Space Grant under contract # 2010-1662-NCSG.

- <sup>1</sup>S. J. Zhang, Y. T. Fei, B. H. T. Chai, E. Frantz, D. W. Snyder, X. N. Jiang, and T. R. Shrout, *Appl. Phys. Lett.* **92**, 202905 (2008).
- <sup>2</sup>S. J. Zhang, Y. Q. Zheng, H. K. Kong, J. Xin, E. Frantz, and T. R. Shrout, *J. Appl. Phys.* **105**, 114107 (2009).
- <sup>3</sup>S. J. Zhang, Y. T. Fei, E. Frantz, D. W. Snyder, B. H. T. Chai, and T. R. Shrout, *IEEE Trans. Ultrason. Ferroelectr. Freq. Control* **55**, 2703 (2008).
- <sup>4</sup>S. J. Zhang, X. N. Jiang, M. Lapsley, P. Moses, and T. R. Shrout, *Appl. Phys. Lett.* **96**, 013506 (2010).
- <sup>5</sup>G. Hunter, J. Wrbanek, R. Okojie, P. Neudeck, G. Fralick, L. Chen, J. Xu, and G. Beheim, *Proc. SPIE* **6222**, 622209 (2006).
- <sup>6</sup>A. Patil, X. A. Fu, P. Neudeck, G. Beheim, M. Mehregany, and S. Garverick, *Mater. Sci. Forum* **600-603**, 1083 (2009).
- <sup>7</sup>D. G. Senesky, B. Jamshidi, K. B. Cheng, and A. P. Pisano, *IEEE Sens. J.* **9**, 11 (2009).
- <sup>8</sup>G. Tortissiera, L. Blanca, A. Tetelina, J.-L. Lachauda, M. Benoitb, V. Conédérab, C. Dejousa, and D. Rebièrea, *Procedia Chem.* **1**, 963 (2009).
- <sup>9</sup>N. A. Riza, M. Sheikh, and F. Perez, *J. Eng. Gas Turbines Power* **132**, 051601-1 (2010).
- <sup>10</sup>T. Aubert, O. Elmazria, B. Assouar, L. Bouvot, and M. Oudich, *Appl. Phys. Lett.* **96**, 203503 (2010).
- <sup>11</sup>T. Huesgen, P. Woias, and N. Kockmann, *Sens. Actuators, A* **145-146**, 423 (2008).
- <sup>12</sup>M. P. da Cunha, T. Moonlight, R. Lad, D. Frankel, and G. Bernhardt, *Proc. IEEE Sens. 2008*, 752 (2008).
- <sup>13</sup>D. J. Frankel, G. P. Bernhardt, B. T. Sturtevant, T. Moonlight, M. P. da Cunha, and R. J. Lad, *Proc. IEEE Sens. 2008*, 82 (2008).
- <sup>14</sup>J. Puigcorbé1, D. Vogel, B. Michel, A. Vilà, I. Gràcia, C. Cané, and J. R. Morante1, *J. Micromech. Microeng.* **13**, 119 (2003).
- <sup>15</sup>K. W. Kim, E. H. Lee, J. S. Kim, K. H. Shin, and B. I. Jung, *Electrochim. Acta* **47**, 2525 (2002).
- <sup>16</sup>R. Vedula, C. S. Desu, S. Tirumala, H. D. Bhatt, S. B. Desu, and K. B. Lee, *Appl. Phys. A* **72**, 13 (2001).
- <sup>17</sup>J. A. Thiele and M. P. da Cunha, *Sens. Actuators, B* **113**, 816 (2006).
- <sup>18</sup>J. A. Thiele, and M. P. da Cunha, *IEEE Trans. Ultrason. Ferroelectr. Freq. Control* **52**, 545 (2005).
- <sup>19</sup>J. G. Lisoni, J. A. Johnson, J. L. Everaert, L. Goux, H. V. Meeren, V. Paraschiv, M. Willegems, D. Maes, L. Haspelslagh, D. J. Wouters, C. Caputa, and R. Zambrano, *Integr. Ferroelectr.* **81**, 37 (2006).
- <sup>20</sup>L. Starck, U.S. Patent No. 5,572,081 (5 November 1996).
- <sup>21</sup>T. Ochiai, *Jpn. J. Appl. Phys.* **37**, 1964 (1998).
- <sup>22</sup>J. M. Kubler, E. Amherst, and M. D. Insalaco, U.S. Patent No. 5,512,794 (30 April 1996).
- <sup>23</sup>K. Kishi, Y. Ooishi, H. Noma, E. Ushijima, N. Ueno, M. Akiyama, and T. Tabaru, *J. Eur. Ceram. Soc.* **26**, 3425 (2006).